LUMINESCENCE BIOTECHNOLOGY

Instruments and Applications

Edited by

Knox Van Dyke
Christopher Van Dyke
Karen Woodfork

CRC PRESS

Boca Raton London New York Washington, D.C.

Library of Congress Cataloging-in-Publication Data

Luminescence biotechnology : instruments and applications / edited by Knox Van Dyke, Christopher Van Dyke, Karen Woodfork.
p. cm.
Includes bibliographical references and index.
ISBN 0-8493-0719-8 (alk. paper)
1. Luminescent probes. 2. Luminescence immunoassay. 3. Luminescence spectroscopy. I. Van Dyke, Knox, 1939- II. Van Dyke, Christopher. III. Woodfork, Karen.

TP248.25.L85 .L86 2001
660.6′028--dc21 2001043471

Visit the CRC Press Web site at www.crcpress.com

International Standard Book Number 0-8493-0719-8
Library of Congress Card Number 2001043471
Printed in the United States of America 1 2 3 4 5 6 7 8 9 0
Printed on acid-free paper

Section VI

Luminescent Imaging

36 Detection Systems Optimized for Low-Light Chemiluminescence Imaging

Mark A. Christenson

CONTENTS

36.1 INTRODUCTION

The luciferase enzyme has provided a powerful tool to examine biological processes within living organisms. By exploiting the ability of this protein to catalyze light emission from a substrate, biological researchers can examine gene expression within a cell, tissue, or whole organism, and measure local ATP release or monitor protein–protein interaction in the cell. Since the stoichiometry of the reaction is one photon emitted per one substrate converted, the light levels produced can be extremely low under some experimental conditions. This chapter describes the current state of the art in imaging technology and the optimization of the imaging conditions required to detect and accurately measure extremely low light level chemiluminescence emission from a variety of biological model systems.

36.2 THE METHOD

The key to good low-light chemiluminescence imaging is to have the best possible signal-to-noise (S/N) ratio for a given number of emitted photons. To achieve the best S/N ratio, the measured signal should be maximized while the all the noise contributions during the measurement should be minimized.[1,2] We can isolate the approach into three different components; the generation of photons from the source, the collection of photons by the optics, and the measurement of photons by the detector. We can then define the signal per pixel (S) as follows:

$$S = \text{Photons emitted from a source} * \text{Collection Efficiency} * \text{Detection Efficiency} \quad (36.1)$$

0-8493-0719-8/02/$0.00+$1.50

Similarly, the total noise per pixel, N, can be separated into terms describing contributions from the source, the optics, and the camera:

$$N = (N_P^2 + N_B^2 + N_C^2)^{1/2} \tag{36.2}$$

where
N_P = photon shot noise
N_B = noise from the background light collected by the optics
N_C = noise from the camera

The S/N measurement will describe the quality of the data collected. The ideal condition for imaging is where the background photon noise and the camera noise are eliminated completely, leaving the inherent noise of the measured photon signal as the only source of noise. This is called "shot noise"-limited imaging and the S/N ratio can be described as follows:

$$\text{S/N (shot noise limited)} \approx \text{Signal}/N_P = \text{Signal}/\text{Signal}^{1/2} = \text{Signal}^{1/2} \tag{36.3}$$

As the signal increases, the S/N also increases in proportion to the square root of the measured signal. In practice, shot noise–limited imaging can be very difficult to achieve, but the discussions in this chapter will focus on optimizing the imaging setup to approach this limit. Given optimized conditions, the researcher will be able to see extremely low light chemiluminescent signals and accurately measure their magnitudes.

The source of photons for chemiluminescence imaging is the breakdown of the luciferin substrate that is catalyzed by the luciferase enzyme. Maximizing the number of photons emitted from the cells or tissue of interest is an important issue, requiring an understanding of the different luciferase enzymes, the levels of that enzyme within a cell or tissue, the ATP levels, the substrate concentration, and the local oxygen levels.[3] Methods of increasing the photon emission rate from targets will not be addressed in this chapter. Nevertheless, the experimentalist should understand the factors affecting the photon generation rate *in situ* because this will affect the overall signal dynamics.

To examine the efficiency of light collection, we need to consider each of the two basic configurations for imaging chemiluminescence—microscope-based imaging and macroscopic imaging. The former is used for high-resolution, single-cell experiments, whereas the latter is used primarily for bulk target imaging like tissues or whole plants. Let us consider each of these in turn.

36.3 MAXIMIZING LIGHT COLLECTION THROUGH THE MICROSCOPE

In chemiluminescence imaging, the microscope should be set up to eliminate all excess optical elements since every interface results in a net reduction in photon number. Every surface that is coated with an antireflection coating will still lose approximately 1% of the light, while uncoated optics can lose 5% or more. The optimization should include the removal of all dichroic beam splitters and filters from the emission pathway. The user should choose the optical path in the microscope that minimizes the number of optical elements prior to the camera port, for example, the bottom port that is now found on the newer-generation inverted microscopes.

The main function of the objective in chemiluminescence imaging is to collect the maximum amount of light possible from the sample. The key measure of the ability of an objective to collect light is its numerical aperture (NA). The NA is defined as follows:

$$\text{NA} = n_0 \sin\theta \tag{36.4}$$

where n_0 = refractive index of the medium between the lens and the sample and θ is the half angle of light cone collected by the lens through the medium.

The larger the NA of the objective, the more light is collected. In fact, the amount of light collected is proportional to the NA,[2] so small changes in NA can have large effects on the results.

Another factor affecting the measurement is the magnification. For a tenfold increase in magnification, the signal will be spread out over a 100-fold larger area so the net intensity per pixel will be reduced by 100-fold. Therefore, one should use an objective that gives the highest NA-to-magnification ratio. In fact, the light-gathering power (LGP) of an objective can be described as follows:[4]

$$\text{LGP} = 10{,}000 * (\text{NA}/\text{Magnification})^2 \tag{36.5}$$

Therefore, if the specimen can be visualized at sufficiently high resolution at 40× magnification, it would be better to use the 40× objective, which has an NA of 1.3 instead of a 100× objective with an NA of 1.4. Since resolution in chemiluminescence imaging tends to be limited by the diffusion of the luciferase during the typical long exposures, the user would do well to use the lower-power objective in most cases.

It may also be possible to select for an objective that has the highest throughput at the peak emission of the chemiluminescent substrate to achieve superior results.[5] In addition, the user should carefully clean any dirt, oil, or other residue from the objectives according to the manufacturer's recommended procedures. The microscope should be set up to direct 100% of the light to the camera port when measurements are to begin.

36.4 MAXIMIZING LIGHT COLLECTION THROUGH A PHOTOGRAPHIC LENS

In macroscopic imaging, a camera is mounted over the target and the light is collected through a standard F-mount-type lens (for charge-coupled devices, or CCDs, with >1 in. diagonal) or a C-mount type lens (for CCDs with <1 in. diagonal). The lens should have the highest light collection efficiency possible, which is specified by the lens f-number. The f-number is defined as follows:[6]

$$\text{f-number} = \text{lens focal length}/\text{entrance pupil diameter} \tag{36.6}$$

and

$$\text{NA}_{\text{lens}} \approx (2 * \text{f-number})^{-1} \tag{36.7}$$

Because the NA_{lens} is inversely related to the f-number, then the best light collection will be accomplished using the lens with the smallest possible f-number. In the case of standard F-mount lenses, the Nikkor 50-mm focal distance lens (Nikon USA, Melville, NY) with an f-number of 1.2 is recommended. For a standard C-mount lens, the Universe Kogaku 25-mm focal distance lens (Universe Kogaku, Oyster Bay, NY) with an f-number of 0.95 is recommended.

The relative light-collecting ability of one lens can be compared with another by taking the inverse ratio of the f-numbers squared. As an example, comparing two lenses with f-numbers of 0.95 and 1.2 on the same target:

$$\text{Light Collection Ratio} = 1.2^2/0.95^2 = 1.6 \tag{36.8}$$

So the f/0.95 lens would collect 1.6 times as much light as the f/1.2 lens.

One trick that can be exploited to increase the light-gathering ability of the lens is to add a macro ring or an extender tube to the back of the lens. The effect of this action can be predicted from the relationship of focal length to image and object distances from the lens:[6]

$$1/\text{focal length} = (1/\text{object to lens}) + (1/\text{image to lens}) \tag{36.9}$$

Note: This thin lens formula is valid for thick lenses when 1° and 2° principal points are used as the internal lens reference points for measuring distance.

Adding the macro ring causes an increase in the image-to-lens distance. Since the focal length of the optic is fixed, this lens movement is compensated for by a reduction in the object-to-lens distance. This means that the object can be brought closer to the lens surface when a macro ring or extender tube is used. By bringing the target closer to the lens, there are two effects. First, the solid angle of light collected from a point source in the field of view is increased, enhancing sensitivity. Second, the object is magnified to a higher degree, which can be very useful for smaller targets. The higher magnification will spread out the signal, reducing the intensity at each pixel, but this can be compensated for by increasing the binning level on the CCD (see discussion below).

36.5 MAXIMIZING THE NUMBER OF DETECTED PHOTONS

Now that the experimental setup has been optimized to deliver the highest number of photons to the detection system, it would be senseless to throw away all this work with a low-sensitivity detector. The efficiency with which the camera measures a signal, the camera detection efficiency, can be described by the following formula:

$$\text{Detection Efficiency} = \text{QE} * \text{Pixel Area} * \text{Time} \tag{36.10}$$

This means that the total signal can now be described as:

$$S = \text{Photon Flux Density} * \text{QE} * \text{Pixel Area} * \text{Time} \tag{36.11}$$

where the photon flux density (PFD) is defined as the number of photons per unit area per unit time arriving at the detector.

The PFD is the combined photon emission rate from the source and the collection efficiency of the optics as discussed above. Once the photons arrive at the camera, the most dominant factor in determining the signal size is the quantum efficiency (QE) of the CCD. The QE is defined as the fraction of incoming photons that actually generate a signal in the CCD and this number is a function of the wavelength of light hitting the CCD. For visible wavelengths of light, the energy level of the photon is only sufficient to generate a single excited-state electron in the CCD so the stoichiometry of electrons out to photons in is 1:1. For very energetic photons, such as X rays, each detected photon can generate multiple excited-state electrons.

The transfer of the photon energy into an excited-state electron occurs within a region of the CCD called the "depletion zone." To create this zone, a defined voltage is applied to surface gate structures on the CCD. These gate structures define the pixel boundaries in one dimension, whereas buried implants define the pixel boundaries in the other dimension.[7] Although necessary to create the pixel and to move charge across the CCD, the overlying gate structures cause a reduction in the QE over a range of visible wavelengths as a result of a combination of reflection and absorption.

To compensate for this kind of loss, CCD manufacturers have introduced a series of innovations. One approach is to use a semitransparent gate structure that allows more of the short wavelengths to reach the depletion zone. Kodak has introduced a series of blue-enhanced CCDs that use indium-tin-oxide in place of silicon oxide for one of the gate lines on each pixel. This enhances the CCD QE throughout the 380- to 580-nm region of the spectrum (Figure 36.1).

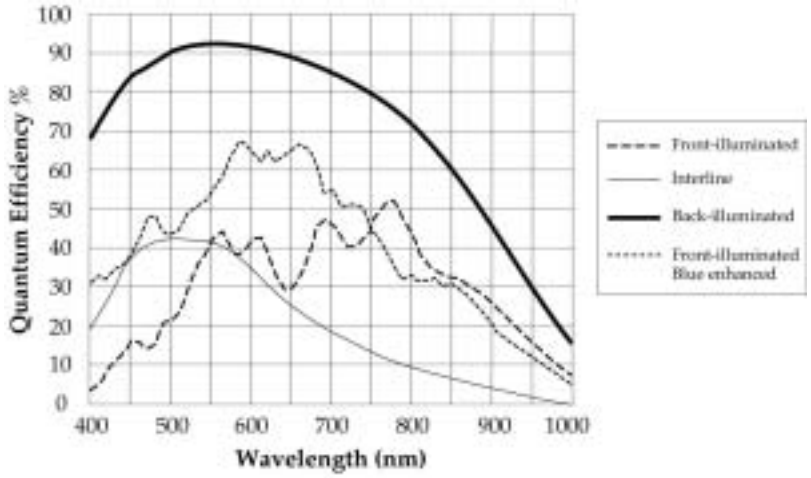

FIGURE 36.1 Quantum efficiency profiles of various CCD types. A comparison of the quantum efficiencies of several CCD types across the visible spectrum is provided. The quantum efficiency represents the number of photons that are converted to measurable signals in the CCD itself.

A unique approach employed in the Sony interline-type CCDs is the use of a photodiode-like sensor to collect the light, but a CCD-like element to store the signal. The net effect is very high QE, but a low area to collect the signal because of the need to place a light-impermeant mask over the storage region on each pixel. The low area of collection is partially compensated for by using a single or double microlens structure on each pixel to focus light onto the photosensitive region.

The most effective means of increasing the net QE is back-illumination, but it is most difficult to accomplish. Back-illuminated (BI) CCDs are produced by turning the CCD over and etching away the supporting silicon substrate to expose the depletion zone. This exposed surface is then layered with an antireflection coating optimized for the visible region of the spectrum. In this configuration, the BI CCD can often achieve quantum efficiencies in excess of 90% for light of approximately 600 nm wavelength.

Figure 36.1 shows the QE profiles of standard front-illuminated (FI), blue-enhanced front-illuminated (BE-FI), interline (IL), and back-illuminated (BI) CCDs. Comparing the QE profiles, it is clear that the BI CCDs have the highest QE of all the sensor types across the whole visible spectrum.

Because QE is a function of wavelength, the actual conversion efficiency of a real signal will depend on the intersection area of the emission wavelength profile of the chemiluminescent substrate and the QE curve of the CCD sensor. For luciferin, the emission maximum wavelength is 560 nm, where the BI CCD has an effective QE of 92%.

Once one has a detector with the optimal QE, the signal intensity will be a function of the cross-sectional area of the pixel: the larger the pixel, the larger the signal. In addition to collecting more light, larger pixels allow for a higher dynamic range. Since the sensor dynamic range is defined as the largest measurable signal divided by the readout noise specification, having a larger "bucket" to hold more charge allows for dynamic ranges that go from 4095 gray levels (12 bits) all the way to 65,565 gray levels (16 bits). There is a fundamental trade-off, however, in that increasing the pixel size reduces the spatial resolution that is achievable with the CCD.

Another approach that can be utilized to increase pixel area in a scientific-grade camera is the software-selectable on-chip binning feature. This allows the user to run the camera at a variety of resolutions and sensitivities. For example, collecting an image at 2×2 binning will yield four times the signal as compared with the unbinned state. Similarly, when 3×3 binning is selected, the user

obtains nine times the unbinned signal. By using on-chip binning, the user also limits the noise in the signal by having one readout event per nine pixels.

The advantage of on-chip binning to S/N can be demonstrated as follows. Assume there are two units of signal per pixel and two units of noise per pixel, a condition that would not allow the user to collect meaningful data at full resolution. Now reading out a 3×3 pixel region yields the following:

$$\text{S/N (unbinned)} = \text{Signal/Noise} = 2/2 = 1$$

By reading out the 3×3 region unbinned and then combining the signal in software after the readout, we have the following S/N:

$$\text{S/N (software binning)} = (\text{Sum of the Signals})/(\text{Sum of the squares of the noise terms})^{1/2}$$

$$= 9 * 2/(9 * 2^2)^{1/2} = 3$$

If instead, we bin all the pixels in a 3×3 region we have only one readout event for all the accumulated signal and hence only one noise term to consider:

$$\text{S/N (binned } 3 \times 3) = (9 * 2)/2 = 9$$

So we can see that there is an increase in the S/N that is equal to the square root of the number of pixels binned when on-chip binning is used vs. software-based binning after full-resolution readout. In this example, some form of binning (hardware or software) would be required to see any significant measurement at all.

The other variable under the control of the user is the exposure time. For signals that are linear with time, an exposure that is two times longer will generate a signal that is two times larger since the CCD camera produces extremely linear data over its full 65,000 gray level range. When the signal itself is not linear, such as in the case where the enzyme activity plateaus early and then begins to decrease over time, the extended exposure will give a net increase in signal, but it will not be proportionally higher. For chemiluminescence imaging, there are a variety of luciferase-type molecules and each has a distinct activity-vs.-time curve and the user should measure the enzyme kinetics *in situ* if quantitative information is desired. Eventually, there will be a point of limited return from a longer imaging period due to drop off in the signal. This should be determined empirically from the preparation under study.

36.6 ELIMINATING NOISE SOURCES

As discussed above, the noise sources of a measurement include the photon shot noise, the background signal noise, and the camera noise. The photon shot noise is inherent to the light signal itself and is equal to the square root of the number of photons measured. So, for 100 measured photons, the associated shot noise would be ±10 while for 10,000 measured photons the associated shot noise would be ±100. This noise term cannot be altered and its contribution can only be minimized by measuring more photons. For many chemiluminescence experiments, there are a limited number of photons that can be measured.

The background signal arises from contaminating stray light entering the optical system. This signal can be eliminated if the contaminating light sources are constant in space and in time. However, the noise associated with this background signal cannot be removed from the data and serves to reduce the overall S/N_T in the measurement. The magnitude of the background noise equals the square root of the background signal. Minimizing this noise source is one of the most

critical factors for successful detection of a faint chemiluminescence signal. To suppress this background light, the microscope must be insulated exceedingly well from stray light.

If all the light is directed to the camera port, there is no need to worry about light coming from the oculars. The main light leakage, therefore, comes via the objective during the integration time. To keep the contaminating light to a minimum, a black foam core material can be used to frame a black box around the microscope, with the seams sealed by a double layer of black tape. The setup also requires a door or access panel to allow the introduction of a sample to the microscope stage. Alternatively, a small, dark chamber can be constructed that covers the sample and blocks light entry into the objective of the inverted microscope.

In addition to the above measures, the room lights should be kept off and all major sources of light should be eliminated. This involves masking light leaks around doors and windows, turning off the computer monitor (or running the computer from an adjacent room) and using black tape to cover light-emitting diodes on equipment in the room. It is also a good idea to use dark clothing that does not have lots of whiteners that can reflect stray light back toward the microscope.

It is easy to measure the background noise in the experimental setup by running a control, such as a dish of cells without the luciferin substrate. Starting with shorter exposures and lower binning ratios, light leaks can be measured and systematically eliminated. Once most of the obvious light leaks have been blocked, a measure of the background noise is made. The easiest way to measure this noise is to use a program that can perform statistics on an image and report back the standard deviation of the signal across the whole field of view. If the value of this standard deviation is close to that standard deviation of a bias image (exposure time set to 0 so no light hits the CCD), then the data should be close to the limit of detectability allowed by the digital camera (see discussion below on measuring noise sources).

For macroscopic imaging, the sample is usually placed into a black box environment where all extraneous photons are excluded by the light tightness of the chamber. In practice, light tightness is a relative term since we have found that some commercial boxes produced for higher-level chemiluminescence signals are not sufficiently dark for the very low light chemiluminescence signals that can be measured by a high-performance digital camera. These boxes can often be made "darker" by sealing the seams with black RTV compound (Dow Corning) or a wide strip of black electrical tape. Also, the camera mount must have an efficient O-ring-type seal (preferably a double O-ring) to prevent light leaking in from the top.

In addition to the light tightness, a dark box should have a wide door with easy sample access. There should be movable stage that can be adjusted with the door closed and the sample platform should be large enough to accommodate multiple target types including multiple petri dishes as well as whole plants and animals. One example of such a dark box is shown in Figure 36.2.

This now brings us to camera-derived noise terms. These include the camera electronic readout noise and the dark current noise in the CCD itself.

$$N_C = (N_R^2 + N_D^2)^{1/2} \tag{36.12}$$

where N_R = readout noise and N_D = dark current noise.

The readout noise arises from the requirement to amplify and measure the small amounts of charge that are generated in the CCD. This is the area where a camera manufacturer uses its expertise in electronic design to minimize the absolute noise level during readout. Often this involves the use of double-correlated sampling techniques, well-isolated electronic circuits, use of high-quality electronic components, and other careful design elements.

For scientific-grade BI CCDs, a major factor influencing the readout noise is the speed at which the analog to digital converter (ADC) is operated. As the amplifier on the CCD is driven faster, the readout noise increases. A tenfold increase in readout rate causes a doubling of the readout noise. Conversely, slowing down the readout rate decreases the noise. For optimal operation,

FIGURE 36.2 Dark box imaging system. An example of a dark box setup along with the LN-cooled VersArray 1300B camera that is used to collect chemiluminescence images. During operation, the camera is mounted on the top of the box via a light-tight seal. The box allows macroimaging of chemiluminescence via a movable stage that can be focused from the outside.

scientific-grade BI CCDs are typically run with a dual ADC configuration; the fast ADC (typically at a 1 megapixel per second rate) is used for setup and focusing, while the slower ADC is used for optimal data collection (typically at a 100 kilopixel per second rate). The lowering of readout noise with slower readout rates eventually reaches a plateau, so systems are rarely used with readout rates much slower than 50 kilopixels per second.

When using a CCD to integrate a signal over time, the user must be aware of the presence of a background signal that grows over time. This background signal is called the dark current and it arises from the thermal energy within the CCD sensor itself.[7] Because of defect structures within the CCD, the thermal energy of the CCD is sufficient to create electron–hole pairs within the pixel well, which results in a signal that is indistinguishable from the photon-derived signal. The rate of dark current accumulation is a function of temperature, so lowering the temperature of the CCD reduces the dark current rate (Figure 36.3). As a rule of thumb, the dark current is lowered by a factor of 2 for every 7° drop in CCD temperature. Some scientific-grade BI CCDs have a substantial dark current rate at room temperatures and high-performance cooling is required to lower the rate to acceptable levels.

For moderate suppression of dark current, a multistage thermoelectric Peltier-type device is used in conjunction with forced-air cooling. The Peltier device transfers heat from one side of the stack to the other side when the unit is electrically powered. This heat is then dispersed by air as it crosses a thermal reservoir or heat block. This type of cooling can produce cameras that run down to −50°C or more, depending on the size of the CCD being used.

For the ultimate in dark current suppression, the CCD can be lowered to −100°C or more using liquid nitrogen (LN)-based cooling mechanisms. In this type of camera, the LN is in thermal contact with a heat block that is bonded to the CCD. The LN pushes the temperature of the CCD downward and stabilization is achieved by adding a small heater to the heat block to keep the temperature

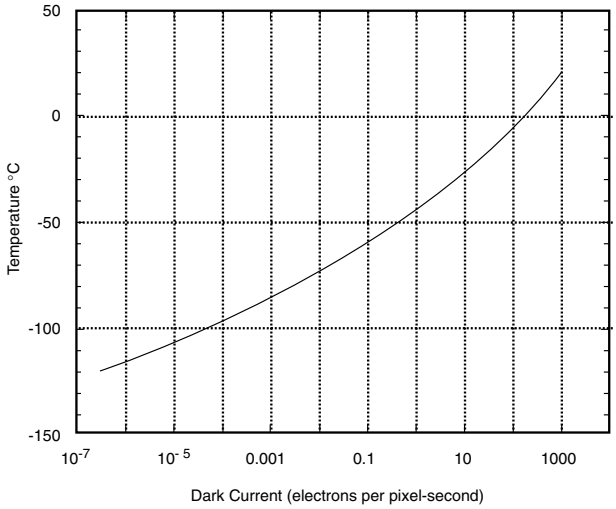

FIGURE 36.3 Dark current as a function of temperature. As the temperature of the CCD is lowered, the dark current rate continually decreases. To achieve the ultralow dark currents desired for chemiluminescence imaging, the CCD should be cooled to the −100°C level or lower.

regulated to within 50 millidegrees of the desired temperature. Under LN cooling, the BI CCDs can be kept to dark current rates that are totally negligible even for exposures of up to 20 min with moderate to high binning. This ultralow cooling is a hallmark of the highest-performance BI cameras that are used for extended integration on the CCD.

36.7 HOW TO MEASURE NOISE LEVELS

The procedure to measure noise levels is fairly straightforward. To measure the readout noise on a system, one can program the camera for a 0-s exposure and then collect three images. Subtract the second and third images on a pixel-by-pixel basis and perform a statistical analysis on the resulting image. The standard deviation of the values in the subtracted image should be divided by 1.414 (square root of 2) since we are deriving the data from a subtraction-based method. The net result will be the root mean square (rms) readout noise in counts.

Similarly, to measure noise due to stray light, collect three images over a time span similar to the desired exposure time, using the same binning as in the experimental measurements but with no sample present. Now subtract the second and third images and measure the standard deviation across the image. As above, divide this number by 1.414 and the result will be the rms noise due to background light and the readout noise combined.

To separate out the background noise from the readout noise, use the total noise formula (Equation 36.2) and the camera noise formula (Equation 36.12). Solving for the background noise (assuming that there is no dark noise due to deep cooling and that there is no signal present):

$$N_B = (N_T^2 - N_R^2)^{1/2} \tag{36.13}$$

where N_R = readout noise. By using this measurement, it is now possible to determine the level of background noise. Ideally, this noise should be reduced to the level of readout noise to ensure that the imaging system can measure the smallest possible chemiluminescent signal.

36.8 A NOTE ON COSMIC RAY–INDUCED SIGNALS

When measuring a very weak signal, obtaining the maximum S/N with a cooled CCD requires binning of the CCD and integration on the CCD for a period of time that can approach minutes. Both of these conditions (large area, large time), however, also increase the probability of detecting of background signals generated by cosmic rays. These background signals appear as very high local signals or spikes against a backdrop of constant low signal. They are caused by secondary particles that are created by cosmic rays entering the atmosphere.[1]

There is no way to prevent the cosmic events from appearing, but lowering the exposure time or reducing the binning will minimize the number of pixels affected by the spurious signal. This approach will limit the signal size and may not be the preferred route. Alternatively, these spikes can be removed by applying a median filter[8] to the image with a neighborhood size of around 5. This will result in some smoothing of the data in the image, but chemiluminescence images often do not have sharp features because of the diffuse distribution of the luciferase and the need to measure a signal over seconds to minutes, which tends to homogenize any localization of the signal that may be present. One other approach is to interpolate across the peaks to remove them. Ideally, this should be done with a two-dimensional interpolation to approximate the true background signal.

36.9 THE IDEAL CAMERA

The discussion above can now help us to craft the ideal system for chemiluminescence imaging. It should have the best collection optics available as measured by NA and magnification (microscope based) or by f-number (macro-imaging). The collection optics should be isolated from all extraneous light sources such that a control exposure under the standard experimental conditions produces noise in the image that is limited by the camera and not by the contaminating light; that is, the background noise should not be any higher than the camera readout noise.

To achieve the best possible signal conversion, the CCD should be of the BI type with peak QE values around 90% in the wavelengths of interest. To eliminate all dark current noise, the CCD should be cooled to −100°C or more. The camera should be equipped with dual ADCs to allow higher-speed operation for setup and focusing and slower-speed operation for low noise and optimal data collection.

The camera should also support on-chip binning capabilities to optimize signal vs. resolution for each experiment. The on-chip binning allows signal collection before readout and therefore optimizes the S/N of the measurement. The system should include easy-to-use software that controls all the features of the camera and presents the data in an easy-to-interpret fashion.

Combined with an environment that is appropriately shielded from light, a camera with these features will allow the experimentalist to image the most-light-starved chemiluminescence preparations, ranging from single cells under the microscope to whole organisms under macroscopic imaging conditions. For experimental conditions where the luciferase levels are much higher, it is sometimes possible to use camera systems which have a lower performance level. In these cases, however, it will be critically important to verify system performance on a realistic sample to ensure adequate sensitivity for the task at hand.

36.10 EXAMPLES OF CHEMILUMINESCENCE IMAGING

Bioluminescence resonance energy transfer (BRET) imaging can be used to measure the proximity of a luciferase–luciferin complex and a green fluorescent protein (GFP) molecule within a cell.[9] When the two protein partners are sufficiently close, the luciferase–luciferin complex donates its energy to the GFP molecule by nonradiative resonance energy transfer, resulting in GFP emission in the absence of illumination. The signals emitted from single cells are extremely low and can be virtually impossible to measure using most camera systems. The Princeton Instruments LN-cooled

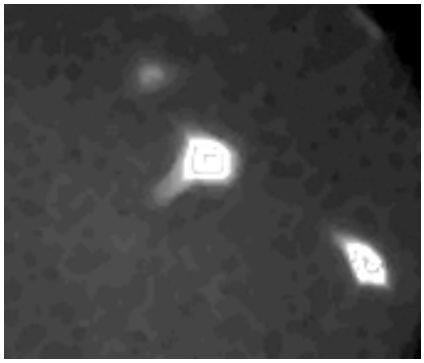

FIGURE 36.4 Example of single-cell BRET imaging. BRET imaged in single COS-7 cells, using *Renilla* luciferase and EYFP as reporters. Images were collected on an inverted microscope using a 40×, 1.3-NA objective. The luciferin was added 10 s before imaging. Exposures were 5 min in length with 6×6 binning. (Data are from the laboratory of Dave Piston, Vanderbilt University.)

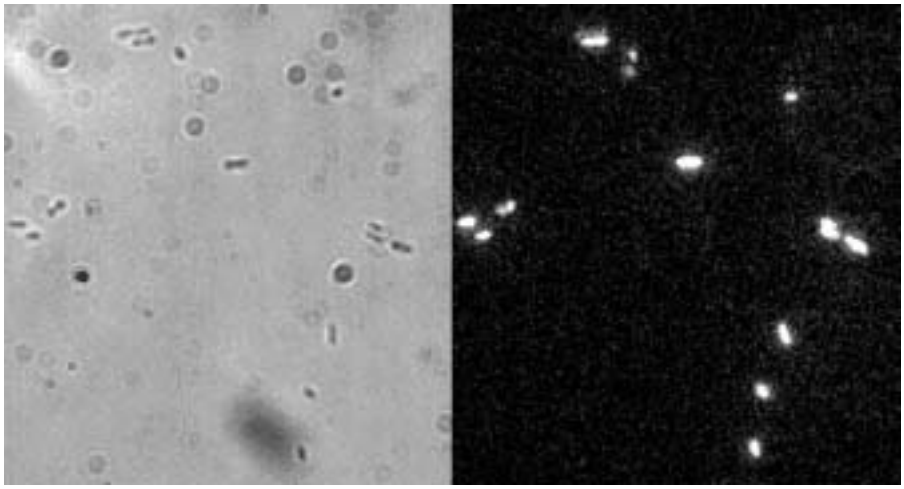

FIGURE 36.5 (Color figure follows p. 266.) Bacterial chemiluminescence imaged through the microscope. Natural bacterial chemiluminescence imaged through the microscope (100× lens, 1.3 NA) using a VersArray 1300B LN-cooled CCD camera system. The image on the left is a brightfield reference image and the image on the right is a bioluminescence image of *Vibrio harveyi* (2.5-min exposure). (Data were taken by Irina Mihalcescu in the laboratory of Stan Leibler, Princeton University.)

VersArray 1300B camera was used to collect the BRET images as shown in Figure 36.4 (Dave Piston laboratory, Vanderbilt University).

Another example of microscope-based chemiluminescence imaging is the characterization of endogenous luciferase activity in chemiluminescent bacteria. Individual bacteria can be imaged over time using the cryogenically cooled VersArray 1300B camera to monitor natural fluctuations in the luciferase under different growth or nutritional states. Figure 36.5 shows robust *Vibrio harveyi* chemiluminescence when examined on the single cell level (Stan Leibler laboratory, Princeton University).

One of the most common macroscopic imaging applications of chemiluminescence is the characterization of plant gene expression levels. The gene activities can be examined in response to a variety of factors such as light, pathogens, or phytohormones. Alternatively, bacterial chemiluminescence can be used as a tracer for infection of plant tissue. An example of this latter type

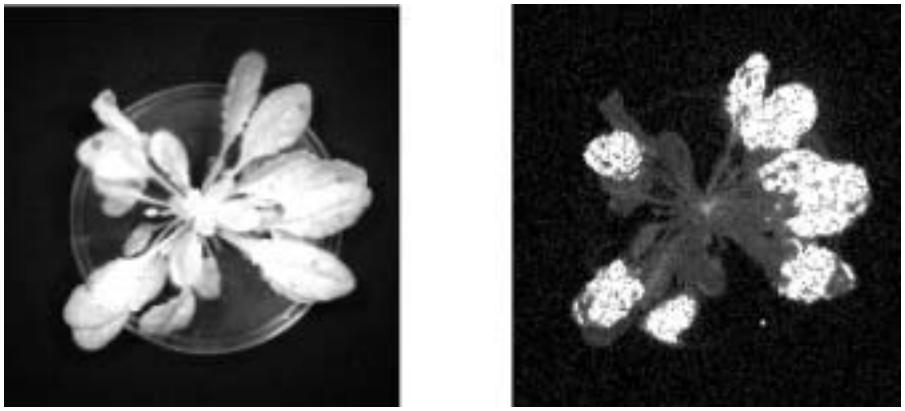

FIGURE 36.6 (Color figure follows p. 266.) Plant chemiluminescence image. Bacteria expressing luciferase were used to infect *Arabidopsis* plants and then whole plants were examined. The blue represents a very low signal, whereas the white represents a high signal. A brightfield reference image is shown on the left and the chemiluminescence image is shown on the right. (Data are from Dr. Jian-Min Zhou, Kansas State University.)

of imaging is shown in Figure 36.6, where *Arabidopsis* leaves were infected with different levels of bacterial pathogens expressing luciferase and imaged on in a black box environment using the LN-cooled VersArray 1300B system (Jian-Min Zhou laboratory, Kansas State University).

Clearly, the doors are now open to more creative and challenging experiments using the luciferase protein as a biomarker in living cells and whole organisms. As researchers become aware of the possibilities now open to them, we should begin to see a whole host of studies published demonstrating real-time changes in gene expression that were previously thought impossible to measure.

REFERENCES

1. Talmi, Y., Intensified array detectors, in *Charge-Transfer Devices in Spectroscopy,* Sweedler, J. W., Ratzlaff, K. L., and Denton, M. B., Eds., VCH Publishers, New York, 1994, chap. 5.
2. Christenson, M. A., The application of scientific-grade CCD cameras to biological imaging, in *Imaging Neurons,* Yuste, R., Lanni, F., and Konnerth, A., Eds., Cold Spring Harbor Laboratory Press, Cold Spring Harbor, NY, 2000, chap. 6.
3. Sala-Newby, G. B., Kendall, J. M., Jones, H. E., Taylor, K. M., Badminton, M. N., Llewellyn, D. H., and Campbell, A. K., Bioluminescent and chemiluminescent indicators for molecular signalling and function in living cells, in *Fluorescent and Luminescent Probes for Biological Activity,* Mason, W. T., Ed., Academic Press, New York, 1999, chap. 17.
4. Inoué, S., *Video Microscopy,* Plenum Press, New York, 1986, chap. 5.
5. Keller, H. E., Objective lenses for confocal microscopy, in *Handbook of Biological Confocal Microscopy,* 2nd ed., Pawley, J. B., Ed., Plenum Press, New York, 1995, chap. 7.
6. *RCA Electro-Optics Handbook,* RCA Solid State Division, Lancaster, PA, 1974, chap. 12.
7. Sims, G. R., Principles of charge-transfer devices, in *Charge-Transfer Devices in Spectroscopy,* Sweedler, J. W., Ratzlaff, K. L., and Denton, M. B., Eds., VCH Publishers, New York, 1994, chap. 2.
8. Russ, J., *The Image Processing Handbook,* 3rd ed., CRC Press, Boca Raton, FL, 1999, chap. 3.
9. Xu, Y., Piston, D. W., and Johnson, C. H., A bioluminescence resonance energy transfer (BRET) system: application to interacting circadian clock proteins, *Proc. Natl. Acad. Sci. U.S.A.,* 96, 114, 1999.

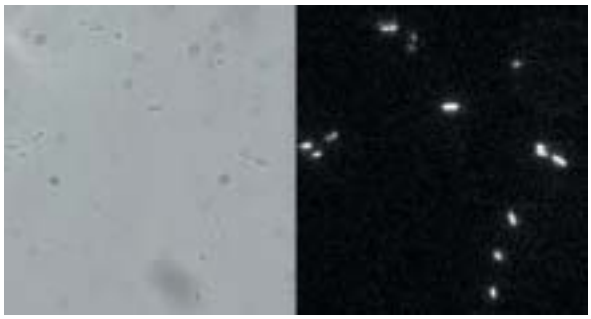

COLOR FIGURE 36.5 Bacterial chemiluminescence imaged through the microscope. Natural bacterial chemiluminescence imaged through the microscope (100× lens, 1.3 NA) using a VersArray 1300B LN-cooled CCD camera system. The image on the left is a brightfield reference image and the image on the right is a bioluminescence image of *Vibrio harveyi* (2.5-min exposure). (Data were taken by Irina Mihalcescu in the laboratory of Stan Leibler, Princeton University.)

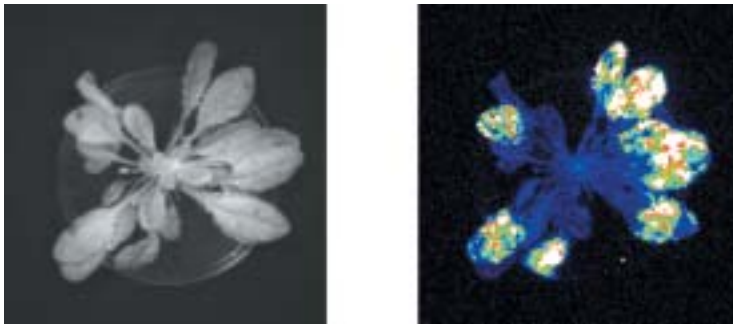

COLOR FIGURE 36.6 Plant chemiluminescence image. Bacteria expressing luciferase were used to infect *Arabidopsis* plants and then whole plants were examined. The blue represents a very low signal, whereas the white represents a high signal. A brightfield reference image is shown on the left and the chemiluminescence image is shown on the right. (Data are from Dr. Jian-Min Zhou, Kansas State University.)